ENSO-Related Interannual Variability of Temperature and Salinity in the Upper Tropical Pacific Ocean during 2005-2006

Qiuxia Wu[@] and Yonghong Yin

[@]Corresponding author address: Dr. Qiuxia Wu, State Key Laboratory of Severe Weather, Chinese Academy of Meteorological Sciences, No.46 South Avenue, Zhongguancun, Haidian District, Beijing 100081, China. Email address: halenmona@gmail.com

MOTIVATION:

1) Spatial distributions of temperature and salinity determine the upper ocean thermodynamic states, which shows a corresponding variation associated with ENSO cycle.
2) The previous ocean observations, such as the TAO/TRITON moored buoy, drifting buoy, ship-of-opportunity XBT and satellites, can not provide a satisfactory coverage in terms of time and space. For the first time, the Argo profiling float project allows continuous monitoring of temperature and salinity in the upper 2000 m of the ocean in near-real time (Gould et al., 2004).
3) Aims: To investigate the observed details of the 2005/2006 ENSO-related variation of temperature and salinity in the entire tropical Pacific Ocean to improve the understanding of ENSO formation mechanism, with the available Argo profile datasets.

DATA and METHOD

- The real-time quality controlled and delayed mode temperature and salinity of Argo profiling floats. (ftp://ftp.ifremer.fr/ifremer/argo/geo/pacific_ocean)
- Cubic-spline functions (201 standard pressure levels extending from 5 to 2000 db, with vertical interval of 10 db at 10 to 2000 db and 5 db at depths shallower than 10 db)
- Potential temperature for the estimates of ILD (UNESCO1983 empirical formula (Fofonoff and Millard, 1983); the equation of state for seawater of Gill (1982) and Bryden (1973)).
- The isothermal layer depth (*ILD*) :The depth where the potential temperature (*PT*) is equal to the sea surface potential temperature (*SSPT*) minus 0.5℃ (Monterey and Levitus 1997).

$$ILD = Z_{(PT = SSPT - 0.5)}$$

, Where Z means the depth. (De Boyer Montegut et al.,2007)

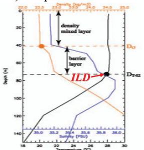

Indicating the vertical motions in the thermocline. (Upward: $\frac{\partial ILD}{\partial t} < 0$, Downward: $\frac{\partial ILD}{\partial t} > 0$)

- The dynamic height (*DH*) refers to the pressure associated with a column of sea water, defined as follows: $DH(p_1, p_2) = \int_{p_1}^{p_2} \delta(T, S, p)dp$

Where p_1 and p_2 are two reference pressure levels, δ is the specific volume anomaly from a standard specific volume determined at a salinity of 35 psu, a temperature of 0℃, T is the temperate, S is the salinity, and p is the pressure.

Referring to vertical displacements of sea level:
- Ascend: $\frac{\partial T}{\partial t} > 0$, $\frac{\partial S}{\partial t} < 0$
- Descend: $\frac{\partial T}{\partial t} < 0$, $\frac{\partial S}{\partial t} > 0$

Indicating cumulative effects of the Temperature/Salinity variations in the vertical direction.

SSTA and Argo profiles' spatial distribution

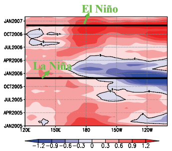

Figure 1. The temporal-longitudinal section of SSTA along the EQ during Jan 2005 to Feb 2007. (A moderate La Niña reaches its mature phase in December 2005 and then a moderate El Niño develops and reaches its mature phase in December 2006 (McPhaden, 2008))

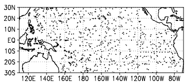

Figure 2. The spatial distribution of Argo profiles in December 2005, illustrating a horizontal resolution of roughly 3 degree.

TEMPERATURE

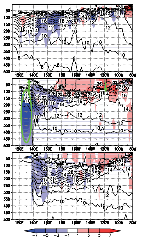

Figure 3. The zonal sections above 500db pressure level along 10° N (upper panel), the equator (middle panel) and 5° S (lower panel). The contour represents the temperature in December 2006 with interval of 2° C; the difference in temperature is defined by subtracting the temperature value in December 2005 from that in December 2006, and the areas with magnitude larger than 1° C are filled in with color. Superimposed thick lines with closed and open circle represent the isothermal layer depth (ILD) in December 2005 and December 2006, respectively.

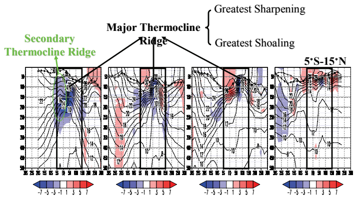

Figure 4. As in Fig. 3, except for the meridional sections along 140° E, 180° E, 140° W and 100° W (From the left to the right panels).

- The major variation of temperature is trapped in the sharp thermocline, and the greatest subsurface temperature variation is found at 5ºS-15ºN, associated with the shoaling and sharpening of the thermocline.
- The vertical motions in the thermocline due to Kelvin/Rossby waves plays a key role in the thermocline-trapped temperature variation
- Worthwhile noting, the greatest cooling on the equatorial Pacific western boundary might be due to a strong upwelling (maybe the strongest upwelling in the tropical Pacific Ocean), which need to be checked by the future works.

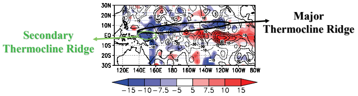

Figure 5. The map for the variation of surface dynamic height (DH) referred to 500dbar due to the temperature variation, isothermal layer depth (ILD) , defined by subtracting the value in December 2005 from that in December 2006. The area with the magnitude of the DH variation larger than 5 dyn cm is filled in with color, and the superimposed contour represents the ILD variation with the interval of 10 m and the contour with magnitude smaller than 10 m is not shown.

- When the greatest warming occurs along the equatorial central and eastern Pacific, the greatest cooling is found along the major thermocline ridge at about 5ºN-15ºN and the secondary thermocline ridge on the equatorial Pacific western boundary, associated with the greatest shoaling and sharpening of the thermocline.
- The asymmetric distribution of the subsurface cooling with respect to the equator could be thought to be associated with the asymmetric shape of the thermocline; that is, there exist the major thermocline ridge at about 5ºN-15ºN and the secondary thermocline ridge on the equatorial Pacific western boundary.
- Along the thermocline ridge, the greatest shoaling of the thermocline causes the nearest subsurface cold water to the sea surface and acts together with the greatest sharpening (Corresponding to the strongest static stability: $-\partial T / \partial p$) to permit the greatest response of the subsurface ocean to the atmospheric forcing.
- According to the subsurface ocean memory mechanisms (Wang, 2001; Wang and Picaut, 2004), the thermocline ridges at about 5ºN-15ºN and on the equatorial Pacific western boundary could be crucial regions for ENSO phase transition.

SALINITY

In the tropical Pacific Ocean, the salinity variation is also associated with ENSO cycle on interannual time scales.

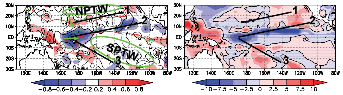

Figure 6. The map for the variation of the sea surface salinity (SSS), (Evaporation – Precipitation) and the surface dynamic height (DH) referred to 500 dbar due to the salinity variation. Left: The SSS variation is defined by subtracting the Argo salinity value in December 2005 from that in December 2006, and the area with magnitude lager than 0.2 psu is filled in with the shade of color. The superimposed contour represents the surface DH variation with magnitude larger than 1.25 dyn cm, defined by subtracting the difference in the DH between December 2006 and December 2005 estimated using the WOA2005 annual mean salinity data from that estimated using the observed Argo salinity data. The superimposed thick solid (red) and dashed (green) contours respectively represent 34.6 psu in December 2005 and December 2006. Right: E-P field in kg/s/m^2 is obtained from the Comprehensive Ocean Atmosphere Data Set (COADS), and the variation of E-P is defined by subtracting the value in December 2005 from that in December 2006 (Positive value: E>P; Negative value: E<P). The thick solid lines with mark 1, 2 and 3 represent the cross sections of Figure 7, respectively.

- The overall distribution pattern of the surface DH variation is similar to that of the SSS variation, indicating that the major variation of salinity is confined in the surface isothermal layer. Moreover, the greatest freshening is found in the surface isothermal layer over the major and secondary thermocline ridges.
- The SSS variation is due to the advection and the external forcing terms (Evaporation - Precipitation).

$$\frac{\partial S}{\partial t} = \underbrace{-\vec{V} \bullet \nabla S}_{\text{Advection}} + \underbrace{E - P}_{\text{Forcing}}$$

- On the southern flank of the high-salinity North Pacific Tropical Water (NPTW), the increased SSS occurs due to the southward movement of the NPTW (Shown by the southward displacement of the contour of 34.6 psu), and the increased dryness (E-P>0).
- Along the ITCZ, including the eastern edge of the western Pacific warm pool (WPWP), the strong freshening, due to severe rainfall (E-P<0), is found there and causes SSS to decline. (Johnson et al. 2002; McPhaden, 2008)
- In the southeastern part of the SPCZ, the increased SSS occurs, due to the increased dryness (E-P>0).

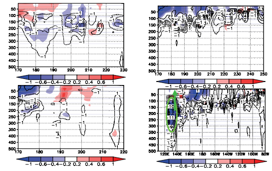

Figure 7. The vertical sections of the salinity variation above 500 db pressure level along the southern margin of the North Pacific Tropical Water (solid line 1 in Fig. 6, upper left panel), the northern margin of the South Pacific Tropical Water (solid line 2 in Fig. 6, upper right panel), the SPCZ (solid line 3 in Fig. 6, lower left panel) and the equator (lower right panel). The area with the magnitude of the salinity variation larger than 0.2 psu is filled in with the shade of color. The superimposed contour with the interval of 1 ℃ represents the temperature variation, and the contour with magnitude smaller than 1 ℃ is not shown. The temperature and salinity variations are defined by subtracting the value in December 2005 from that in December 2006, respectively.

- Contrary to temperature, the major variation of salinity is indeed confined in the surface isothermal layer, with the greatest freshening occurring in the surface isothermal layer over the major and secondary thermocline ridge
- The variation of subsurface salinity is trapped in the thermocline and is synchronized with the major variation of subsurface temperature, due to the vertical motions associated with the subsurface Kelvin/Rossby waves in the thermocline.
- Worthwhile noting, like a greatest thermocline-trapped cooling on the equatorial Pacific western boundary, a great thermocline-trapped freshening is also found there, due to a strong upwelling, maybe the strongest upwelling in the tropical Pacific Ocean.

CONCLUSION

- The greatest sharpening and shoaling of thermocline exists in the major thermocline ridge at 5°N-15°N and the secondary thermocline ridge on the equatorial Pacific western boundary.
- Due to the greatest sharpening and shoaling of thermocline, the major and secondary thermocline ridges is favorable for the strong air-sea interaction (Hermes and Reason,2009; Vialard et al., 2009), indicated by the greatest thermocline-trapped cooling and the greatest surface-isotermal-layer-confined freshening, and could play a key role in ENSO phase transition.
- Worthwhile noting, on the equatorial Pacific western boundary, there maybe exist a strongest upwelling in the tropical Pacific Ocean, which might be a deciding factor in the ENSO phase transition.
- The future works is focused to check if the major and secondary thermocline ridges is crucial regions for ENSO phase transition.

REFERENCES

Bryden, H. L., 1973: New polynomials for thermal expansion, adiabatic temperature gradient, and potential temperature of sea water, *Deep-Sea Res.*, 20, 401–408.

De Boyer Montégut, C., J. Mignot, A. Lazar, and S. Cravatte (2007), Control of salinity on the mixed layer depth in the world ocean: 1. General description, *J. Geophys. Res.*, *112*, C06011, doi:10.1029/2006JC003953.

Fofonoff, N. P., and R. C. Millard Jr., 1983: Algorithms for computation of fundamental properties of seawater, *UNESCO Tech Papers in Marine Sci.*, No. 44, 53 pp.

Gill, A. E., 1982: *Atmosphere-Ocean Dynamics*, Academic Press, 662 pp.

Gould, J., et al., 2004: Argo profiling floats bring new era of in situ ocean observations, *Eos Trans*, *AGU*, 85(19), doi:10.1029/2004EO190002.

Hermes, J. C., and Reason, C. J. C. 2009. The sensitivity of the Seychelles–Chagos thermocline ridge to large-scale wind anomalies. – ICES Journal of Marine Science, 66: 000–000.

Johnson G. C., B. M. Sloyan, W. S. Kessler, and K. E. McTaggart, 2002: Direct measurements of upper ocean currents and water properties across the tropical Pacific Ocean during the 1990's, *Progress in Oceanography*, 52(1), 31–61.

McPhaden, M. J., 2008: Evolution of 2006-2007 El Niño: the role of intraseasonal to interannual time scale dynamics, *Adv. Geosci.*, 14, 219-230.

Monterey, G., and S. Levitus, 1997: *Seasonal Variability of Mixed Layer Depth for the World Ocean*, NOAA Atlas NESDIS 14, U.S. Gov. Printing Office, Wash., D.C., 96 pp. 87 figs.

Vialard, J., and Coauthors, 2009: Cirene: Air—Sea Interactions in the Seychelles—Chagos Thermocline Ridge Region. *Bull. Amer. Meteor. Soc.*, 90, 45–61.

Wang, C., 2001: A unified oscillator model for the El Niño-Southern Oscillation, *J. Climate*, 14, 98-115.

Wang, C., and J. Picaut, 2004: Understanding ENSO physics – A review, in *Earth's Climate: The Ocean-Atmosphere Interaction*, Geophysical Monograph Series, Volume 147, edited by C. Wang, S.-P. Xie, and J. A. Carton, pp. 21-48, AGU, Washington, D.C.